Lab on a Chip

Dynamic Article Links

Cite this: *Lab Chip*, 2011, **11**, 2693

www.rsc.org/loc

PAPER

A microfluidic system for fast detection of mitochondrial DNA deletion

Chen-Min Chang,[a] Li-Fang Chiu,[b] Pei-Wen Wang,[b] Dar-Bin Shieh*[bc] and Gwo-Bin Lee*[d]

Received 14th April 2011, Accepted 31st May 2011
DOI: 10.1039/c1lc20317g

This study reports an integrated microfluidic system capable of automatic extraction and analysis of mitochondrial DNA (mtDNA). Mitochondria are the energy production and metabolism centres of human and animal cells, which supply most of the energy for maintaining physiological functions and play an important role in the process of cell death. Because it lacks an effective repair system, mtDNA suffers much higher oxidative damage and usually harbours more mutations than nuclear DNA. Alterations of mtDNA have been reported to be strongly associated with mitochondrial dysfunction, mitochondria-related diseases, aging, and many important human diseases such as diabetes and cancers. Thus, an effective tool for automatic detection of mtDNA deletion is in great need. This study, therefore, proposed a microfluidic system integrating three enabling modules to perform the entire protocol for the detection of mtDNA deletion. Crucial processes which included mtDNA extraction, nucleic acid amplification, separation and detection of the target genes were automatically performed. When compared with traditional assays, the developed microfluidic system consumed fewer samples and reagents, achieved a higher mtDNA extraction rate, and could automate all the processes within a shorter period of time (150 minutes). It may provide a powerful tool for the analysis of mitochondria mutations in the near future.

Introduction

Mitochondria are regarded as the energy powerhouse of human and animal cells. They can synthesize adenosine triphosphate (ATP) mainly through oxidative phosphorylation processes[1,2] to provide energy for sustaining a wide spectrum of cellular physiological functions.[3] Alterations in mitochondrial DNA (mtDNA) have been reported to be highly associated with degenerative diseases of the nerves and muscles, the aging process, and various common human diseases such as cancers and diabetes.[4] Sequencing of human mtDNA has been completed,[5,6] which provided a foundation for investigating many human diseases and aging processes.[7–9] Besides, the heteroplasmy that exists in mitochondria genomes is often closely associated with clinical symptoms of the affected individuals.[10,11]

Among mitochondria-related diseases, chronic progressive external ophthalmoplegia (CPEO) and Kearns–Sayre syndrome (KSS) have been recognized to be associated with large-scale deletion of mtDNA.[12,13] For instance, various types of mtDNA mutations were found in the muscle of the CPEO patients and the 4977 base-pair (bp) deletion was present in the predominant genotype. Besides, mitochondrial respiratory functions were found to degrade in human tissues during the aging process.[14] Furthermore, the efficiency of oxidative phosphorylation in human livers[15] and muscle tissues[16,17] declined with the aging process. 4977-bp deletion has been recognized to be one of the most common mtDNA mutations in the tissue samples of an aging population.

mtDNA forms a double-stranded circular structure with a total length of 16 569 bps (Fig. 1(a-1)).[18] This genetic information is transferred to offspring through maternal inheritance.[19,20] The mtDNA mutation rate is about 10–20 times higher than that of nuclear DNA[21] because of a less sophisticated DNA repair mechanism, lack of histone protein protection, and proximity to the inner membrane of the mitochondria that is susceptible to attack from free radicals.[22,23] The deletion occurs when the mtDNA is attacked during replication (Fig. 1(a-2)).[24–28] Since the replication of mtDNA is asymmetric, if the mtDNA breaks during replication, the mtDNA will release the broken DNA fragment between the repetitive flanking sequence fragments (Fig. 1(a-3) and 1(a-4)). Note that the 4977-bp common deletion usually occurs between the replication origins of the heavy strands and light strands.

Recently, micro-electro-mechanical-system (MEMS) and microfluidic technologies have been widely explored for automation of miniature biomedical devices and systems. MEMS can

[a]*Department of Engineering Science, National Cheng Kung University, Tainan, 701, Taiwan*
[b]*Institute of Oral Medicine, National Cheng Kung University, Tainan, 701, Taiwan. E-mail: dshieh@mail.ncku.edu.tw; Fax: +886-6-2766626; Tel: +886-6-2353535 Ext. 5410*
[c]*Department of Stomatology, National Cheng Kung University Hospital, Tainan, 701, Taiwan*
[d]*Department of Power Mechanical Engineering, National Tsing Hua University, Hsinchu, 30013, Taiwan. E-mail: gwobin@pme.nthu.edu.tw; Fax: +886-3-5722840; Tel: +886-3-5715131 Ext. 33765*

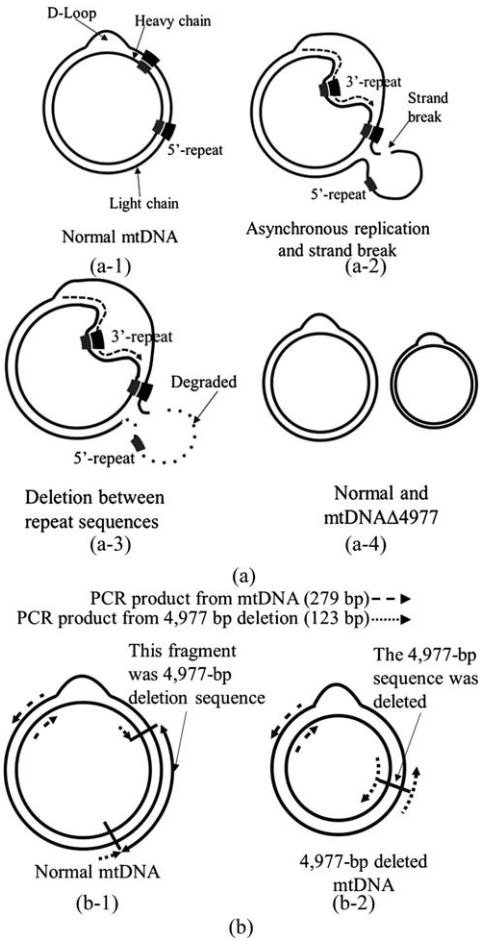

Fig. 1 Illustration of replication and primer design principle for the detection of mtDNA deletion: (a) Illustration of the proposed formation of an mtDNA deletion for replication. (b) Designed DNA primers close to the endpoints of the 4977-bp deletion.

integrate multiple micro-devices to form a lab-on-a-chip such that highly-sensitive detection can be achieved within a short period of time. The major advantages of microfluidic systems include low unit cost, low sample/reagent consumption, portability, automation and disposability.[29–32] Microfluidic devices have been used for applications involving mtDNA. For example, a micro-electrophoresis chip for qualitative analysis of mtDNA was demonstrated.[33] Microchip-based mtDNA extraction has been demonstrated by the current research group by using magnetic beads.[34] However, to the best of the authors' knowledge, this is the first attempt to detect mtDNA deletion by using an integrated microfluidic system.

In this study, the entire process including mtDNA extraction, polymerase chain reaction (PCR) for nucleic acid amplification, separation and detection of the target deletion was performed in a three-dimensional (3D) microfluidic system in an automatic manner. In order to minimize the chip size, several different functional modules were packaged in a vertical layout. Integration of magnetic beads[35,36] with microfluidic technology could allow extraction of the specific mtDNA with a high extraction efficiency. The micro-PCR module amplified the total mtDNA and the specific deleted DNA fragment. Micro-capillary electrophoresis (MCE) was then used to analyze the micro-PCR products to validate and quantify the deletion profile. The microfluidic system consisted of micropumps, a micromixer, microvalves, a micro-PCR module and a MCE module. Compared with conventional assays, the experimental results revealed that this microfluidic system provided a higher extraction efficiency[34] and faster analysis of the deletion profile.

Experimental

2.1 Primer design for mtDNA to examine 4977-bp deletion

From the mechanism of mtDNA 4977-bp deletion, specific mtDNA primers close to the endpoints of the 4977-bp defect, where the deletion occurs between 8470 bp (heavy chain)/8482 bp (light chain) and 13 447 bp (heavy chain)/13 459 bp (light chain) in the mtDNA, can be designed. Since this DNA fragment has a length of 4977 bps, the given PCR elongation time is not long enough to generate amplified products in the non-deleted genome (Fig. 1(b-1)). On the contrary, if the mtDNA deletion occurs, the PCR can amplify the designed DNA fragment with a length of 123 bps (Fig. 1(b-2)), thus enabling quantification of the deleted mtDNA containing both 279-bp and 123-bp fragments when compared to the amount of mtDNA containing only the 279-bp fragments. Briefly, the 279-bp DNA fragment derived from the D-loop region is essential for mtDNA replication and therefore its abundance would reveal the total mtDNA concentration. On the other hand, as the 123-bp fragment could only be amplified in the given limited PCR extension time when mtDNA had 4977-bp deletion, thus the concentration of 123-bp amplicon would represent the concentration of mtDNA with 4977-bp deletion.

2.2 Sample preparation

In order to obtain the total mtDNA from the cultured cells, sample preparation was performed.[37,38] A primary skin fibroblast culture derived from the biopsy samples of CPEO affected patients was maintained in a Dulbecco's Modified Eagle Medium (DMEM) containing 5% fetal bovine serum (FBS), 100 μg ml^{-1} pyruvate and 50 μg ml^{-1} uridine. Osteosarcoma cell line (143B TK-cells) was cultured in 50 ng ml^{-1} ethidium bromide to build up an mtDNA-less human cell line (ρ^o cells). The ρ^o cells were then fused with the CPEO cells to form clones that harbour mtDNA with different proportions of deleted copy (*e.g.*, the cytoplasmic hybrids). After quantification of the deletion profile, the clones with undetectable mtDNA deletion and those with 90% 4977 bps mtDNA deletion were selected for the subsequent experiments. In this study, 1×10^6 cells were used in the extraction module.

2.3 Conventional PCR amplification of mtDNA

For comparison, a PCR analysis was performed in a conventional PCR machine (Bio-Rad iCycler 170-8703). As mentioned previously, there are two mtDNA fragments amplified using 15 μl reaction mixture containing 1 μl extracted DNA, 0.5 μl of 2.5 mM each of dNTP, 1.5 μl of 10× PCR buffer (15 mM $MgCl_2$, 500 mM KCl, 100 mM Tris–HCl, pH 8.8 @ 25 °C and 1% (v/v) Triton X-100), 1 μl of paired primers (0.5 μl of L5604-H5863 and 0.5 μl of L8395-H13494), 0.5 unit of *Taq* DNA polymerase, and

10.5 μl of deionized water. The entire PCR process was performed using the following operating conditions: a first-stage denaturing at 95 °C for 10 minutes, a second-stage with 35 amplification cycles (annealing at 58 °C for 45 seconds, extension at 72 °C for 30 seconds), and a final extension stage at 72 °C for 10 minutes. The PCR amplified products were then electrophoretically separated in a 2% agarose gel using 100 volts in 40 minutes, and then detected by an imaging system (GelDoc® Imaging System, UVP BioSpectrum AC system, USA). A primer pair (L8395 and H13494) was applied to amplify a 123-bp DNA fragment that represented mtDNA with 4977-bp deletion (Table 1). On the other hand, another primer pair (L5604 and H5863) was applied to amplify a 279-bp fragment that represented the total mtDNA.[39] The amplified PCR products were subjected to electrophoresis analysis using a 2% TBA slab-gel with a 100 bp DNA marker (Yeastern Biotech Corp., Taiwan).

2.4 Chip design

Fig. 2(a) illustrates schematically the assembled mtDNA extraction and analysis system. The microfluidic system was composed of three modules, namely, an mtDNA extraction module, a micro-PCR module and a MCE module. All these modules were integrated vertically to form a more compact system such that automatic operation was possible. The mtDNA extraction module consisted of the micropumps for sample injection and the micromixer for the incubation of sample and the magnetic beads (Fig. 2(b)). The micro-PCR module was equipped with microheaters and a micro-temperature sensor to amplify the DNA fragments of interest (Fig. 2(c)). The MCE module was composed of a cross-shaped microchannel to separate and detect the signals of the amplified PCR products (Fig. 2(d)). This vertical layout of the microfluidic system provided the flexibility to integrate several micro-modules with desired functions into a compact microchip system. Note that *via*-holes were designed to transport samples between these modules. The detailed dimensions of the individual components are listed in Table 2.

2.5 Chip fabrication

In this study, a standard photolithography technique was used to fabricate the microchips. Briefly, a SU-8 negative thick photoresist (SU-8-50, MicroChem, Newton, MA, USA) was first spin-coated on a silicon wafer, followed by a two-stage soft baked process (65 °C for 10 minutes and 90 °C for 30 minutes). After an exposure process (500 mJ cm^{-2}), the exposed SU-8 film was post-baked at 65 °C for 5 minutes and 90 °C for 10 minutes to form the molds for the subsequent polydimethylsiloxane (PDMS) replication process, which was used to create the inverse images of the microstructures.[34] The microheaters and the temperature sensors were fabricated by standard photolithographic and metal lift-off processes.[40] The PDMS layers were then mechanically peeled off from the master molds. The PDMS layers and the glass substrate containing the microheaters and the temperature sensors were then treated with an oxygen plasma that bonded them together. Additionally, the three modules (the mtDNA extraction module, the micro-PCR module and the MCE module) were integrated into the microfluidic system using an oxygen plasma pre-treatment.

Table 1 Primers for total mtDNA and 4977-bp deletion

Sample	Gene/annealing temperature	Primers (5′→3′)
Total mtDNA	L5604-H5863 (279 bps)/58 °C	L5604:cactctgcatcaactgaacg H5863:agtccaatgcttcactcagc
4977-bp deletion	L8395-H13494 (123 bps)/58 °C	L8395:caccataattacccccatactcctta H13494:gaggaaagg-tattcctgc-taatgc-3′

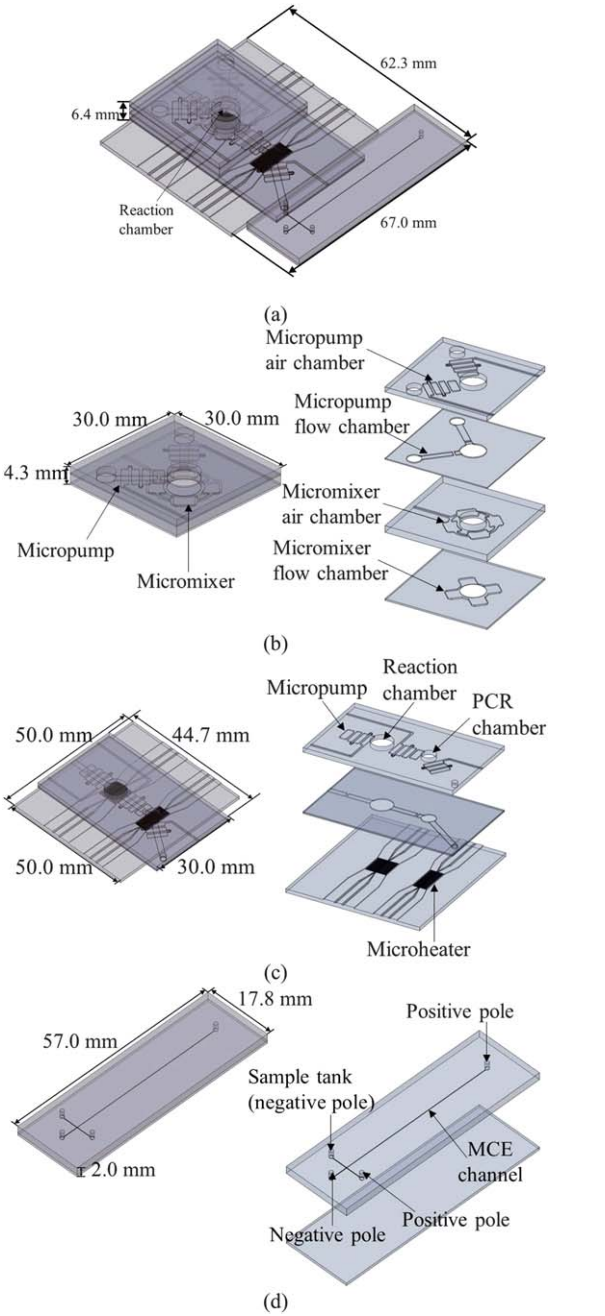

Fig. 2 (a) Schematic illustration of the microfluidic system for mtDNA extraction and analysis. (b) An exploded view of the mtDNA extraction module. (c) An exploded view of the micro-PCR module. (d) An exploded view of the MCE module.

Table 2 The dimensions of the components integrated onto the mtDNA extraction and analysis system (unit: μm)

	Width	Length	Depth
Micropump air chamber	1600	6000	300
Micropump flow channel	1800	—	250
Micromixer air chamber	5200	4000	400
Micromixer flow channel	4300	5000	300
Microheater	7200	7200	250
MCE channel	70	40 000	70
	Diameter		
Reaction chamber	7000		6400

2.6 Experimental setup

Fig. 3 shows the process for mtDNA extraction/analysis and the experimental setup for this study. As shown in Fig. 3(a), extraction of mtDNA was implemented in the reaction chamber after thermal lysis of the cells such that mtDNA can be released from mitochondria (Fig. 3(a-1)). The micropump was then employed to inject the magnetic beads modified with single-stranded DNA (TGG TAT TTT CGT CTG GGG GGT ATG) to bind with the D-loop of the mtDNA in the reaction chamber (Fig. 3(a-2)). The micromixer was then used to thoroughly mix the magnetic beads and the mtDNA to capture the mtDNA (Fig. 3(a-3)). After the incubation process, an external magnet was used to attract the magnetic beads at the bottom of the reaction chamber while the waste solution was pumped out. Then, deionized water (DI water) was injected to perform a washing step such that purified mtDNA can be extracted (Fig. 3(a-4)). Later, the mtDNA-conjugated magnetic beads were injected into another reaction chamber containing the PCR reagents to perform nucleic acid amplification. The designed DNA primers could be used to flank two DNA fragments representing the mtDNA and the 4977-bp deletion, respectively (Fig. 3(a-5)). Finally, the amplified DNA products were transported to the subsequent chamber containing DNA markers for MCE analysis. Under a high electric field, the DNA markers and the amplified DNA fragments migrated at different velocities due to the different sizes of the DNA fragments. Thus the DNA fragments were separated from each other and can be detected by using a laser induced fluorescence system. The signal percentage s of the mtDNA to 4977-bp deletion could be then used to determine the percentage of deletion (Fig. 3(a-6)).

Fig. 3(b) illustrates the experimental setup. Two temperature control units, one compressed air supply unit, six electromagnetic valves (EMVs; S070M-5BG-32, SMC, Japan) and a fluorescent microscope system (BX-41; Olympic, Japan) were used. The compressed air was used to activate the pneumatic micropumps and the micromixer by adjusting the actuation frequency which was regulated by EMVs. When the air entered and filled the air chamber of the micropumps/micromixers, the PDMS membranes would be deflected downwards to drive the fluid forward in the channel, thus generating fluid pumping and mixing. Two temperature control units were used for modulating the reaction chamber temperatures for mtDNA extraction (60 °C) and for micro-PCR amplification (95 °C, 58 °C and 72 °C). The amplified PCR products were separated and detected by employing a high-voltage power supply and a fluorescent microscope system.[41]

2.7 Cell lysis and mtDNA extraction on the mtDNA module

Lysis buffer (50 mM Tris–HCl, 150 mM KCl, 1 mM EDTA, 0.1% Nonidet P-40) and cells were mixed in the mixing chamber for mtDNA extraction. The lysis process was conducted at 60 °C for 15 minutes in a reaction chamber containing 1×10^6 cells in a volume of 300 μl. The magnetic beads were surface-modified with DNA fragments (Dynabeads® MyOne™ Carboxylic Acid, Invitrogen, USA) and were delivered to the chamber. Furthermore, they were free from any nuclear DNA contamination. The incubation process was performed at room temperature for 5 minutes. An external magnetic field of 4000 Gauss was used to attract the beads and deionized water was used in three repeated washings to remove cellular debris. Finally, the extraction sample was re-suspended with 20 μl deionized water. The mtDNA extraction process was performed automatically within 50 minutes.

2.8 Preparation of PCR reagents on the micro-PCR module

The micro-PCR operation was completed within 80 minutes. Mineral oil was used to prevent evaporation of the PCR mixture. 15 μl of PCR reagents contained 0.5 μl of 2.5 mM each of dNTP, 1.5 μl of 10× PCR buffer (15 mM $MgCl_2$, 500 mM KCl, 100 mM Tris–HCl, pH 8.8 @ 25 °C and 1% (v/v) Triton X-100), 1 μl of paired primers, 0.5 unit of *Taq* DNA polymerase, 10.5 μl of deionized water and 1 μl extracted DNA. The operating conditions for the micro-PCR were identical to the traditional PCR protocol described in section 2.3.

2.9 Preparation of the reagents on the MCE module

In order to enhance the separation efficiency of the MCE module, surface modification of the PDMS-based microchannel was conducted prior to usage.[42,43] Briefly, after bonding of the PDMS layers together, the MCE module was thoroughly washed using alcohol, 0.1 M sodium hydroxide (NaOH) and DI water for 5 minutes. Then, the microchannels were treated by using a non-ionic polymer solution (slightly cationic) and poly (ethylene glycol)-*block*-poly(propylene glycol)-*block*-poly (ethylene glycol) (PEG-PPG-PEG) triblock copolymer for 2 minutes. The microchannels were kept in the solution for another 15 minutes before rinsing with DI water. The same process was then performed to coat another anionic polymer solution, poly (acrylic acid) (PAA) polymer. Finally, the microchannels were coated with polymer bilayers repeatedly such that a stable anionic surface property can be observed.

The CE buffer was a mixture of 2% hydroxypropyl methylcellulose (HPMC) in tris–borate–EDTA (TBE) and 1% YO-PRO®-1 fluorescence dyes (Molecular Probes, Inc., USA). Sample injection was performed by applying a voltage of 200 V cm^{-1} for 20 seconds, while separation was conducted under a voltage of 250 V cm^{-1} applied for 3 minutes. For comparison purposes, DNA markers (#SM1103, Ferments, USA) with a concentration of 5 ng μL^{-1} were mixed with the PCR products and separated at the same time in the microchannels. The fluorescent signals were collected using a photomultiplier tube module (PMT; C3830, R928; Hamamatsu Photonics, Japan) downstream of the microchannel (4 cm away from the intersection of the cross-shaped microchannels). Note that the DNA

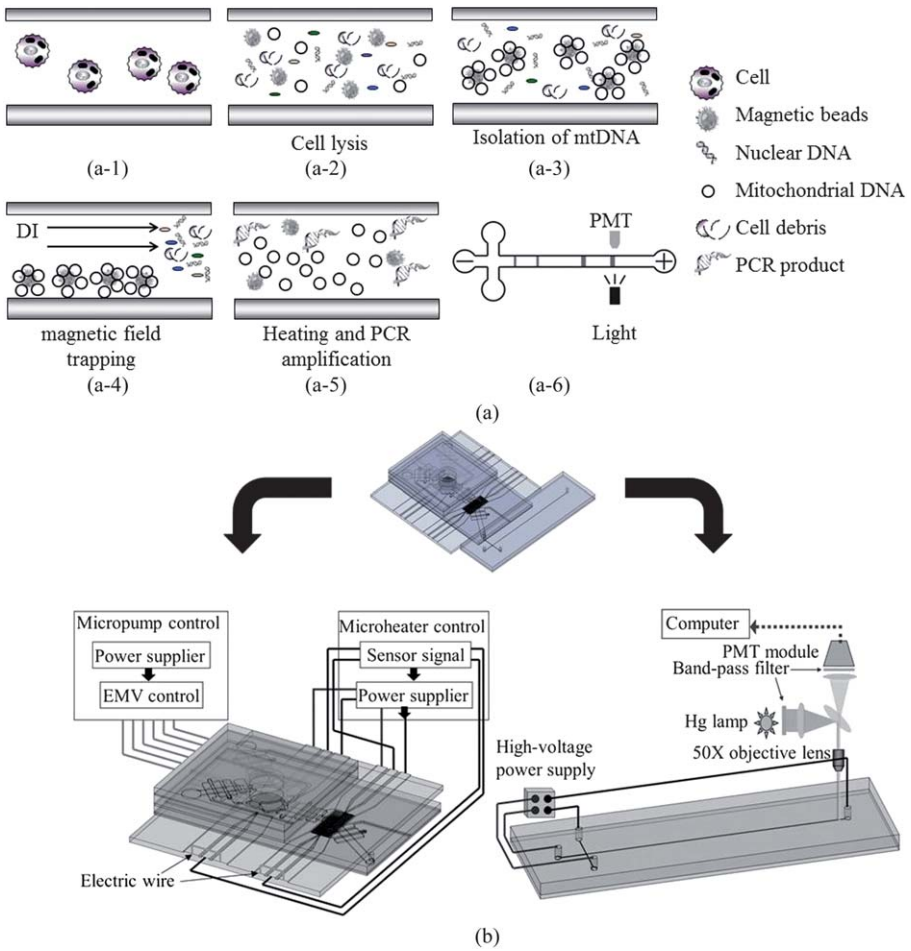

Fig. 3 (a) Illustration of the procedures for extraction and analysis of mtDNA on a microfluidic system. (b) The experimental setup for the mtDNA extraction module, the micro-PCR module and the MCE module.

ladder was spiked in the reagent and stored in the sample tank prior (Fig. 2(c)) to the CE separation.

Results and discussion

3.1 Characterization of the microfluidic system

3.1.1 Characterization of the micropump. The pumping rates of the pneumatic micropump were characterized by measuring the volume of the DI water pumped in the reservoirs after actuating the micropump for 1 minute. Note that the measurements were repeated 5 times to obtain the average pumping rate. Detailed information about the pumping rates can be found in our previous work.[34] It was clearly observed that the pumping rates increased with the increased deflections of the PDMS membranes attributed to increased pneumatic pressures. The maximum pumping rate was about 100 μl min^{-1} when the driving frequency was 25 Hz at 10 psi. This was because the maximum pumping rate at a constant pressure was limited by the restoration of the PDMS membranes. If the driving frequency was too high, the PDMS membranes cannot be restored to their original position and the pumping rate cannot increase but started to decrease. In this study, the micropumps were driven at a frequency of 25 Hz under an applied air pressure of 10 psi such that all transportation processes were finished within a short period of time.

3.1.2 Characterization of the micromixer. In order to characterize the performance of the micromixer, a mixing index was used.[44] Briefly, 250 μl of DI water and 2 μl of blue ink were first loaded in the mixing chamber. Then an image was taken to characterize the mixing performance. Detailed information about the mixing index can be found in our previous work.[34] The experimental results showed that the normalized concentration profile approached a completely mixed state throughout the mixing chamber within a short period of time. For instance, when the pneumatic micromixer was driven at a frequency of 4 Hz and a pressure of 10 psi, the mixing indices before and after mixing were calculated to be 19.6% and 94.7%, respectively, within 0.6 seconds. Note that the higher the applied driving frequency, the less time required to achieve complete mixing in the tested range (from 1 Hz to 10 Hz). However, shear stress increased with the driving frequency, thus increasing the possibility of DNA damage.[45] In this study, a driving frequency of 4 Hz and a pressure of 10 psi were chosen to provide a gentle mixing effect.

3.2 mtDNA extraction

A quantitative measurement of mtDNA extraction was performed using a commercial kit to compare those obtained from our microchip. The extraction time of the commercial kit was

300 minutes; conversely, our microchip assay only took 50 minutes, which was much shorter than the commercial kit. Furthermore, the normalized fluorescent intensity of the real-time PCR products extracted by the commercial kit and our microchip was compared. The results demonstrated that the mtDNA concentration prepared by the microchip was about 1.8 times better than that from the commercial kit. Note that these results were presented in our previous work.[34]

3.3 mtDNA fragment amplification

Fig. 4 shows the separation of amplified mtDNA fragments analyzed by slab-gel electrophoresis and the MCE module. Note that the mtDNA used for traditional and on-chip PCR processes was extracted by the extraction module. Fig. 4(a) shows two cases, one from the PCR results performed in a conventional thermocycler machine and the other from the developed micro-PCR module. Note that lane L is a DNA marker, M represents the normal mtDNA, and D corresponds to the mtDNA containing 4977-bp deletion. The results showed that the amplified products from the micro-PCR module had comparable intensities with that obtained from the conventional PCR machine (120 minutes), indicating that the micro-PCR module (80 minutes) performed DNA amplification more efficiently and within a shorter period of time.

Note that, only the 279-bp DNA fragment was amplified in the normal mtDNA since the PCR extension time did not allow the primer pair to have sufficient time to amplify the 4977-bp fragment. In contrast, when the mtDNA harbours 4977-bp deletion, the PCR enables amplification of a 123-bp fragment flanking the deleted fragment. Thus not only was the 279-bp fragment representing the total mtDNA amplified, but also the 123-bp fragment could be observed. These results revealed that the developed microfluidic system, besides extracting mtDNA, was able to amplify the specific DNA fragments corresponding to the total and the deleted mtDNA using the micro-PCR module.

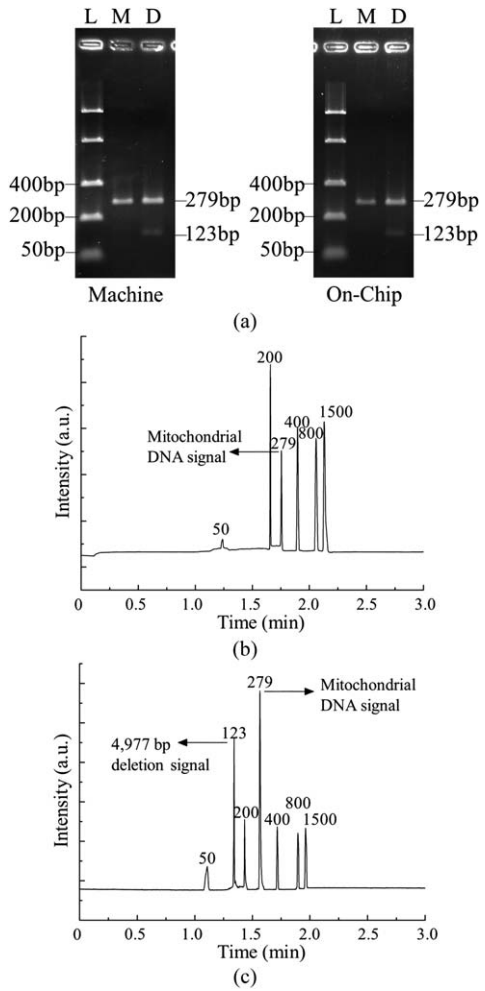

Fig. 4 (a) Slab-gel electropherograms for the amplified mtDNA and DNA fragments from a conventional PCR machine and the developed micro-PCR module. (b) The electropherogram for the normal mtDNA from the developed MCE module. (c) The electropherogram for mtDNA with 4977-bp deletion. The presence of the 123-bp fragment indicates that the mtDNA had a 4977 deletion.

3.4 mtDNA separation and detection

Fig. 4(b) and 4(c) show the MCE separation of the amplified mtDNA products by using the micro-PCR module. The DNA markers and amplified DNA products were mixed in a 1 : 1 volume ratio in the sample chamber of the MCE module in which the microchannel was filled with a mixture of YO-PRO®-1 and HPMC gel. Fig. 4(b) is an electropherogram containing the normal mtDNA and the DNA markers. The 279-bp amplified fragment for the total mtDNA can be easily identified from the markers. It also indicated that the 4977-bp deletion did not occur in this case. In Fig. 4(c), however, the signal representing 4977-bp deletion was clearly observed. Therefore, it was confirmed that the MCE module could detect both the normal and deleted mtDNA successfully.

Patients with mitochondria-related diseases may have significant clinical symptoms if the accumulated mtDNA mutation reaches certain levels in specific tissues.[46] In order to quantify the mutation percentage, mtDNA samples containing different concentrations of 4977-bp deletion were used and analyzed by the MCE module. Note that the mtDNA samples were extracted and amplified by the micro-extraction and micro-PCR module, respectively. Then the samples harboring different ratios of 4977-bp deletion were used to evaluate the MCE detection limit as shown in Fig. 5. In this case, 4977-bp deletion (123-bp) and total mtDNA (279-bp) PCR products were mixed in five different percentages, including 0%, 20%, 40%, 60%, 80%, and 100%. The 4977-bp deletion (123-bp) and total mtDNA (279-bp) PCR products were obtained from two independent PCR reactions. Two different cells harboring normal and high percentage of mutated DNA were lysed separately and then mixed in different ratios. It was clearly observed that the signal from the deleted 123-bp fragment weakened as the percentage of 4977-bp mtDNA deletion decreased, as shown in Fig. 5(b). The amount of mtDNA deletion is reasonably in proportion to the signal intensity of amplicons representing the 279-bp of mtDNA and enables a reasonable measurement of the mutation percentage in the total mtDNA. Note that the variation in the measurements was within 30%. Therefore, the degree of mtDNA deletion can be determined based on the established calibration curve. Note that 4 independent experiments were conducted to get the calibration curve.

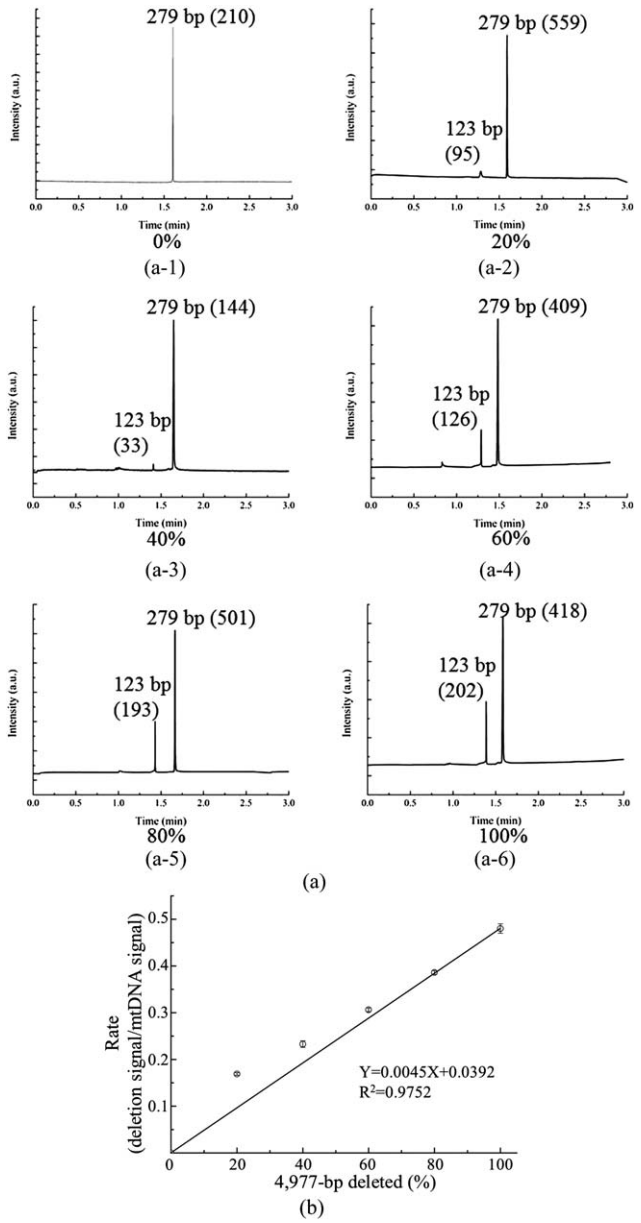

Fig. 5 (a) Electropherograms for mtDNA samples containing different percentages of 4977-bp deletion when separated and detected by the developed MCE module. (b) The relationship between the mtDNA deletion percentage and the signal intensity percentage (123 bps/279 bps).

Conclusion

In this study, an integrated microfluidic system for mtDNA extraction, amplification of target DNA fragments, and detection of amplified PCR products was developed. The mtDNA extraction module, the micro-PCR module and the MCE module were vertically integrated in a microfluidic system by applying three-dimensional packaging. This system utilized magnetic beads to extract and purify mtDNA from cells. The extraction efficiency was found to be superior to the existing method. The extracted mtDNA was then delivered directly to the micro-PCR module by the micropump, where the target DNA fragments were amplified. Finally, the MCE module was used to analyze the mtDNA deletion percentage. The experimental results showed the PCR module could provide a comparable amplification yield when compared to a conventional instrument. The mutation rate of the mtDNA in the samples can be further quantified by measuring the percentage between the amplicon that represents the 4977-bp deletion (123 bps) and that for the total mtDNA (279 bps). Thus, this microfluidic system could be successfully applied to automated mtDNA extraction and analysis. It may provide a promising tool for the early detection and rapid diagnosis of mitochondria-related diseases in the future.

Acknowledgements

The authors gratefully acknowledge the financial support provided to this study by the National Science Council in Taiwan (NSC 99-2221-E-006-043-MY3). The authors also greatly thank Prof. Y. H. Wei for providing mtDNA samples.

References

1 A. R. Fernie, F. Carrari and L. J. Sweetlove, *Curr. Opin. Plant Biol.*, 2004, **7**, 254–261.
2 Y. Hatefi, *Annu. Rev. Biochem.*, 1985, **54**, 1015–1069.
3 G. Attardi and G. Schatz, *Annu. Rev. Cell Biol.*, 1988, **4**, 289–333.
4 R. Luft, D. Ikkos, G. Palmieri, L. Ernster and B. Afzelius, *J. Clin. Invest.*, 1962, **41**, 1776–1804.
5 D. C. Wallace, G. Singh, M. T. Lott, J. A. Hodge, T. G. Schurr, A. M. Lezza, L. J. Elsas and E. K. Nikoskelainen, *Science*, 1988, **242**, 1427–1430.
6 I. J. Holt, A. E. Harding and J. A. Morgan-Hughes, *Nature*, 1988, **331**, 717–719.
7 J. Christodoulou, *Hum. Reprod.*, 2000, **15**(Suppl 2), 28–43.
8 P. F. Chinnery and D. M. Turnbull, *Mol. Med. Today*, 2000, **6**, 425–432.
9 S. Servidei, *Neuromuscular Disord.*, 2002, **12**, 101–110.
10 Y. H. Wei and H. C. Lee, *Adv. Clin. Chem.*, 2003, **37**, 83–128.
11 J. Sastre, F. V. Pallardo and J. Vina, *Free Radical Biol. Med.*, 2003, **35**, 1–8.
12 M. Zeviani, C. T. Moraes, S. DiMauro, H. Nakase, E. Bonilla, E. A. Schon and L. P. Rowland, *Neurology*, 1988, **38**, 1339–1346.
13 J. M. Shoffner, M. T. Lott, A. S. Voljavec, S. A. Soueidan, D. A. Costigan and D. C. Wallace, *Proc. Natl. Acad. Sci. U. S. A.*, 1989, **86**, 7952–7956.
14 Y. H. Wei, *Mutat. Res.*, 1992, **275**, 145–155.
15 T. C. Yen, S. H. Chen, K. L. King and Y. H. Wei, *Biochem. Biophys. Res. Commun.*, 1989, **165**, 994–1003.
16 I. Trounce, E. Byrne and S. Marzuki, *Lancet*, 1989, **333**, 637–639.
17 R. H. Hsieh, J. H. Hou, H. S. Hsu and Y. H. Wei, *Mol. Biol. Int.*, 1994, **32**, 1009–1022.
18 S. Anderson, A. T. Bankier and B. G. Barrell, *Nature*, 1981, **290**, 457–465.
19 R. E. Giles, H. Blanc, H. M. Cann and D. C. Wallace, *Proc. Natl. Acad. Sci. U. S. A.*, 1980, **77**, 6715–6719.
20 N. Howell, P. F. Chinnery, S. S. Ghosh, E. Fahy and D. M. Turnbull, *Hum. Reprod.*, 2000, **15**, 235–245.
21 F. M. Yakes and H. B. Van, *Proc. Natl. Acad. Sci. U. S. A.*, 1997, **94**, 514–519.
22 J. Wanagat, Z. Cao, P. Pathare and J. M. Aiken, *FASEB J.*, 2001, **15**, 322–332.
23 A. A. Johnson and K. A. Johnson, *J. Biol. Chem.*, 2001, **276**, 38097–38107.
24 K. J. Krishnan, A. K. Reeve, D. C. Samuels, P. F. Chinnery, J. K. Blackwood, R. W. Taylor, S. Wanrooij, J. N. Spelbrink, R. N. Lightowlers and D. M. Turnbull, *Nature*, 2008, **40**, 275–279.
25 D. L. Robberson and D. A. Clayton, *Proc. Natl. Acad.Sci. U. S. A.*, 1972, **69**, 3810–3814.
26 I. J. Holt, H. E. Lorimer and H. T. Jacobs, *Cell*, 2000, **100**, 515–524.
27 T. Yasukawa, A. Reyes, T. J. Cluett, M. Y. Yang, M. Bowmaker, H. T. Jacobs and I. J. Holt, *EMBO J.*, 2006, **25**, 5358–5371.
28 G. J. Wang, L. M. Nutter and S. A. Thayer, *Biochem. Pharmacol.*, 1997, **54**, 181–187.

29 B. Ziaie, A. Baldi, M. Lei, Y. Gu and R. A. Siegel, *Adv. Drug Delivery Rev.*, 2004, **56**, 145–172.
30 K. Sato, A. Hibara, M. Tokeshi, H. Hisamoto and T. Kitamori, *J. Chromatogr., A*, 2003, **987**, 197–204.
31 R. Raiteri, M. Grattarola and R. Berger, *Mater. Today*, 2002, **5**, 22–29.
32 N. H. Chiem and D. J. Harrison, *Clin. Chem.*, 1998, **44**, 591–598.
33 P. Taylor, D. P. Manage, K. E. Helmle, Y. Zheng, D. M. Glerum and C. J. Backhouse, *J. Chromatogr., B: Anal. Technol. Biomed. Life Sci.*, 2005, **822**, 78–84.
34 C. M. Chang, L. F. Chiou, C. C. Lin, D. B. Shieh and G. B. Lee, *Microfluid. Nanofluid.*, 2010, **9**, 489–498.
35 K. Y. Lien, C. J. Liu, Y. C. Lin, P. L. Kuo and G. B. Lee, *Microfluid. Nanofluid.*, 2009, **6**, 539–555.
36 M. A. M. Gijs, *Microfluid. Nanofluid.*, 2004, **1**, 22–40.
37 Y. H. Wei, C. F. Lee, H. C. Lee, Y. S. Ma, C. W. Wang, C. Y. Lu and C. Y. Pang, *Ann. N. Y. Acad. Sci.*, 2001, **928**, 97–112.
38 D. B. Shieh, W. P. Chou, Y. H. Wei, T. Y. Wong and Y. T. Jin, *Ann. N. Y. Acad. Sci.*, 2004, **1011**, 154–167.
39 S. A. Mohamed, D. Wesch, A. Blumenthal, P. Bruse, K. Windler, M. Ernst, D. Kabelitz, M. Oehmichen and C. Meissner, *Exp. Gerontol.*, 2004, **39**, 181–188.
40 T. M. Hhieh, C. H. Luo, F. C. Huang, J. H. Wang, L. J. Chien and G. B. Lee, *Sens. Actuators, B*, 2008, **130**, 848–856.
41 C. H. Kuo, J. H. Wang and G. B. Lee, *Electrophoresis*, 2009, **18**, 3228–3235.
42 K. Boonsong, M. M. Caulum, B. M. Dressen, O. Chailapakul, D. M. Cropek and C. S. Henry, *Electrophoresis*, 2008, **29**, 3128–3134.
43 D. Lazos, S. Franzka and M. Ulbricht, *Langmuir*, 2005, **21**, 8774–8784.
44 S. Y. Yang, J. L. Lin and G. B. Lee, *J. Micromech. Microeng.*, 2009, **19**, DOI: 10.1088/0960-1317/19/3/035020.
45 D. H. Triyoso and T. A. Good, *J. Physiol.*, 1999, **515**(2), 355–365.
46 C. D. Berdanier and H. B. Everts, *Mutat. Res.*, 2001, **475**, 169–183.

